北海道大学工学部研究報告
第109号（昭和57年）

Bulletin of the Faculty of Engineering,
Hokkaido University, No. 109 (1982)

LINAC-TOF Neutron Diffraction Experiment on Liquids

Norio OHTOMO*, Yukio TANAKA* and Kiyoshi ARAKAWA**
(Received March 31, 1982)

Abstract

A time-of-flight (TOF) neutron diffraction facility has been developed to carry out structural studies on molecular liquids and solutions, using pulsed neutrons produced by the electron linear accelerator (LINAC) at Hokkaido University. This paper gives a detailed description of the experimental instrumentation together with its resolution and accuracy, and, further, describes the comprehensive data processing procedure including a flow diagram of the data reduction program, which is useful for the analysis of neutron diffraction data on liquids in general.

1. Introduction

Structural studies of liquids, solutions and amorphous materials are most efficiently performed by a TOF neutron diffraction method using the LINAC. The method possesses an advantage over a conventional diffraction method at the reactor in obtaining structure factors for a wide Q-range. Using the experimental setup installed at Hokkaido University, the authors' group has carried out to date a series of TOF neutron diffraction studies on hydrogenous molecular liquids and solutions: water,[1~3] aqueous ionic solutions[2~4] and organic liquid such as acetyl chloride.[5] And, with the aid of a newly devised theoretical procedure of analysis, the diffraction data were analyzed, and detailed knowledge of the liquid structures was obtained. Thus, the LINAC-TOF neutron diffraction method has proved to be a powerful tool for elucidating the structure of liquids and solutions in general.

In the LINAC-TOF neutron diffraction experiment, highly reliable instruments are required and a comprehensive procedure of data processing must be implemented. Some necessary improvements of the instrumental setup have been made in part. Recently, we have improved neutron diffractometer by installing a new neutron counting system, and have obtained a general systematical procedure of data processing. As the result, the quality of the measured data has been raised to a more satisfactory level. The present paper gives a detailed description of the experimental setup together with its resolution and accuracy, and, further, the details of the data

*Department of Atomic Engineering
**Institute of Applied Electricity, Hokkaido University

processing procedures including a flow diagram of the data reduction program.

2. Scattering Fundamentals of the TOF Neutron Diffraction Experiment

Neutron scattering process can be described in terms of the energy transfer $\hbar\omega$ ($\equiv E_0 - E_s$) and the momentum transfer $\hbar\vec{Q}$ ($\equiv \hbar\vec{k}_0 - \hbar\vec{k}_s$), where E_0 and E_s are the incident and scattered neutron energies, respectively, and $\vec{k}_0$ and $\vec{k}_s$ the corresponding wave-vectors. When scattered neutrons are observed at an angle 2θ to the incident beam, the magnitude of $\vec{Q}$ is expressed as

$$Q=\left\{2k_0^2\left[1-\frac{m\omega}{\hbar k_0^2}-\left(1-\frac{2m\omega}{\hbar k_0^2}\right)^{\frac{1}{2}}\cos 2\theta\right]\right\}^{\frac{1}{2}} \qquad (1)$$

For elastic scattering: $E_0=E_s$ (i.e., $\omega=0$) and $|\vec{k}_0| = |\vec{k}_s| \equiv k$,

$$Q=2\,k\sin\theta=\frac{4\pi}{\lambda}\sin\theta, \qquad (2)$$

where $k\equiv 2\pi/\lambda$ and λ is the neutron wavelength. We note that the neutron scattering by liquids, solutions and amorphous materials is uniform in the azimuth.

In the TOF experiment, neutrons arriving at the detector are observed at the fixed angle 2θ at time t after the generation of a neutron burst at time $t=0$, travelling a total flight path, ℓ. Then, the useful conversion expressions are given as,

$$Q=3177\frac{\ell}{t}\sin\theta,\quad t=\frac{72.3\,\ell}{\sqrt{E}}\quad\text{and}\quad \lambda=\frac{0.286}{\sqrt{E}} \qquad (3)$$

where Q is the momentum transfer in Å^{-1}, t the time-of-flight in μs, λ the wavelength in Å, E the energy transfer in eV, ℓ the flight path in m and 2θ the scattering angle in degrees.

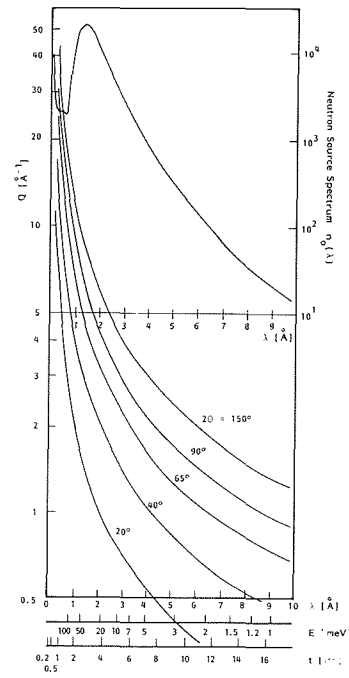

Fig. 1. Neutron source spectrum $n_0(\lambda)$ (H_2O at 293°K) and wavelength λ, energy E and time-of-flight t ranges covered by the spectrum, together with Q-values vs. t (or λ, E) at various scattering angles.

Figure 1 shows the typical wavelength, energy and time-of-flight ranges covered by the burst neutrons. The neutron count-rate time-spectrum consists of an essentially Maxwell-Boltzmann distribution accompanied with the slowing-down specrum ($\propto 1/E$): the spectrum is for neutrons moderated by a water slab ($25\times25\times5\,\text{cm}^3$) at 293°K. Q-values vs. t (or λ, E) at various scattering angles are also given in the figure. The wavelength range covered for an acceptable count-rate of neutrons is from ca. 0.3 Å to 5 Å.

3. Experimental Instrumentations

An instrumental setup used for the LINAC-TOF neutron diffraction experiment is illustrated diagrammatically in Fig. 2. The facility consists of the following subdivisions: pulsed neutron source, TOF neutron diffractometer, neutron counting system and data processing unit, including a temperature control system. A brief discussion of each part will be made below. Detailed specifications are summarized in Table 1.

3. 1 Pulsed Neutron Source

In the LINAC-TOF neutron diffraction experiment, a burst of 45 MeV electrons impinges on a water-cooled heavy metal target and pulsed photo-neutrons are produced through the (γ, n) nuclear reaction in the target. Thereafter, the neutrons are partially moderated by a water slab and become low energy neutrons in the Maxwell-Boltzmann distribution. The neutron yield and mean-emission-time of the pulsed neutron source are important for raising the resolution and accuracy in the TOF diffraction experiment. They are dependent on the operating procedure of the source

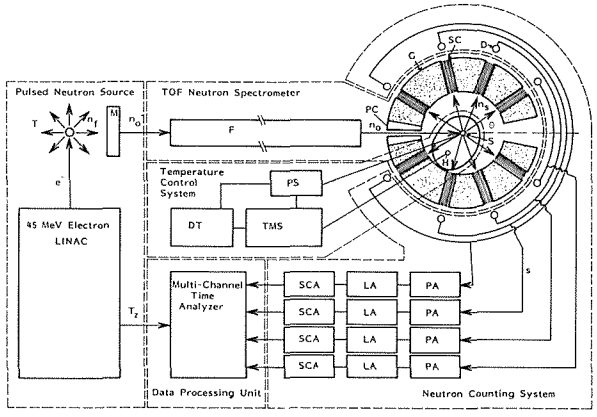

Fig. 2. Schematic diagram of instrumental setup for LINAC-TOF neutron diffraction.
e^- : electron beam, n_f : fission neutrons, n_o' : neutron leakage from the moderator, n_o : incident neutrons, n_s : Scattered neutrons, s : electric signal, T_z : starting trigger, 2θ : scattering angle, T : target (Pb), M : moderator (H_2O), F : flight tube, G : goniometer, PC : pre-collimator, S : sample, SC : Soller collimator, D : detector (^3He), H : heater, PA : preamplifier, LA : linear amplifier, SCA : single channel pulse-height-analyzer, PS : power supply, TMS : thermocouple multipoint selector, DT : digital thermometer.

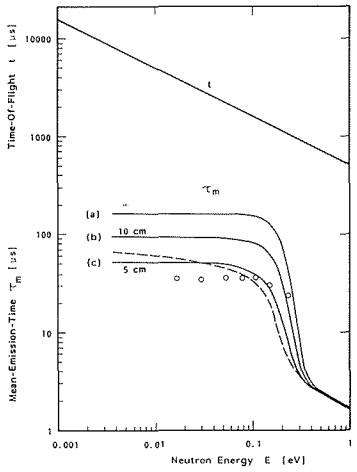

Fig. 3. Time-of-flight of neutrons travelling a total flight path (7.16m), t, and mean-emission-time of source moderator (H_2O at 293°K), τ_m. ——: τ_m calculated by the time moment method,[6] (a) : infinite medium, (b) : slab (10cm thickness), (c) : slab (5cm thickness), ------: τ_m calculated by the time step method,[6,7] o : experimental data for H_2O slab (5cm thickness) at 293°K[6]

Table 1 Specifications of the instrumental setup

[Pulsed Neutron Source]
LINAC
S-band travelling-wave type
electron beam energy
averaged power 3 kW
max. energy >45 MeV
(1 mA peak current)
electron beam current
max. peak current >100 mA
electron pulse
pulse width 0.1, 0.5, 3 μs
repetition rate 10 ∿ 200 μs

Target
water-cooled, Pb and W
dimensions $5 \times 5 \times 5$ cm^3
fast neutron yield 1×10^{12} n/cm^2/s

Moderator
H_2O at room temperature
rectangular $25 \times 25 \times 5$ (or 2.5) cm^3
vessel Al
mean-emission-time 50 μs (λ = 1.8 Å)
4 μs (λ = 0.5 Å)
thermal neutron yield $>4 \times 10^{11}$ n/cm^2/s

[TOF Neutron Diffractometer]
simultaneous measurements at multi-scattering angles
scattering angle variable 20 ∿ 150°

Flight Path
incident (souce-sample) 6.93 m
scattered (sample-detector) 0.23 m

Collimator
pre-collimator slit width 51′
Soller collimator slit width 30′, 38′

[Neutron Counting System]
Detector
Harshaw-made ^{3}He , 10 atm
wall material Al
operating voltage 1700 ∿ 2000 volts
diameter 2.54 cm
effective length 12.0 cm

Electronic Devices
NIM Modules : ORTEC-made
preamplifier Model 142PC
linear amplifier Model 485
discriminator Model 550
low-voltage power supply Model 114
High-Voltage Power Supply
FLUKE-made Model 410B

[Data Processing Unit]
Multi-Channel Time Analyzer
TOSHIBA-made
channel width variable 4 ∿ 20 μs
channel overflow variable
128 ∿ 4096

Computer
HITAC M200H
at Hokkaido University
Computing Center

[Sample Container]
cylindrical shape quartz
internal diameter 10 mm
length 100 mm
wall-thickness ∿ 0.1 mm

[Temperature Control System]
Heating Device : radiation type
Reflector
elliptical-sylindrical shape
material Al
major axis 200 mm
minor axis 176 mm
height 220 mm
Main Heater Rod
diameter 15 mm
length 180 mm
Auxilliary Plane Heater
diameter 70 mm
thickness 10 mm

Thermocouple chromel-alumel

Temperature Control Devices : FLUKE-made
Thermocouple Multipoint Selector
Model Y2001
Digital Thermometer Model 2190A

system, e. g., LINAC, in addition to its shape, dimensions and arrangement of target and moderator, etc. Under the following conditions of LINAC operation, the pulse width of electron beam=3μs and the repetition rate=100 pps, the yield of fast neutrons produced in the target is of the order of 10^{12} neutrons/cm^2/s and the maximum thermal neutron yield at the moderator is more than 4×10^{11} neutrons/cm^2/s (Fig. 1).

The mean-emission-time τ_m can be determined by theoretical and experimental procedures (Fig. 3). Solid curves are the results calculated theoretically by the time moment method.[6] The dashed curve is also a theoretical one obtained for a 5 cm thickness water slab by solving the time-dependent, multi-group, neutron transport equation according to a time step method.[6,7] The open circles are experimental values of τ_m obtained from the time-dependence of monochromatic neutron pulses measured with single crystals.[6]

3. 2 TOF Neutron Diffractometer

In the TOF neutron diffractometer shown schematically in Fig. 2, the neutron intensities scattered in different directions are measured simultaneously, where the scattering angle varies between 20° and 150°. Neutrons scattered in each direction are detected in a bifurcated array of two counters (Fig. 2).

The incident beam of heterochromatic neutrons is collimated by a precollimator, which is made of epoxy-adhesive B_4C powder, after passing through a flight tube set in a shielding wall (heavy concrete). The size of the incident beam is 100mm height × 20mm width at the sample position. The neutrons are scattered isotropically by the liquid sample and the scattered neutrons are detected by the counter at a fixed angle 2θ. The scattered beam is collimated by the Soller collimator composed of parallel Cd-sheets behind the sample. In that collimator, the slit width is designed to be variable and the angular divergence of the slit is 30′ and 38′ at lower and higher scattering angles, respectively, in the present experiment. The slit width of the Soller collimator primarily governs the resolution, and, when the measurement is carried out at a smaller scattering angle, it should be designed to be sufficiently narrower.

3. 3 Neutron Counting System

In order to determine the structure factors for a wide-Q range, the experimental accuracy of the TOF neutron diffraction method must be raised by keeping the measuring time short as well as by keeping the overall background at a minimal level. A "multi-scattering-angle neutron-counting-system" newly installed in our laboratory is in accord with that requirement. The system is constructed out of high-efficient detectors and reliable electronic devices.

The detectors used are Harshow-made ^3He neutron proportional counters, which are filled to a pressure of 10 atm with a gas of ^3He. ^3He utilizes the (n, p) reaction: ${}^3_2He + {}^1_0n \rightarrow {}^1_1H + {}^3_1H + 764\,keV$. The wall of the detector is made of aluminum and its dimensions are follows: the diameter is 2.54 cm and has a sensitive length of 12.0 cm. In addition to the higher energy resolution (~6%), the 10 atm counter has an excellent sensitivity to neutrons and it is virtually "black" to thermal neutrons. The operating voltage of the detector ranges from 1700 to 2000 volts in the preferred gas multiplication region of 10 to 50. The electronic devices used are nuclear instrumental electronic modules obtained from ORTEC Inc. The signal to noise ratio is very excellent and electric noises are negligible. Thus, the optimal neutron counting system is quite useful for the improvement of the experimental accuracy.

3. 4 Data Processing Unit

The output pulses from two detecters at the same scattering angle are combined and fed through electronic devices into a data processing unit. A main part of the unit is a multi-channel time analyzer (USC-1 Model 10 obtained from TOSHIBA Inc.) which is described in three parts: a time-to-digital converter with maximum 4096 channels, 4096 channels permanent memory unit accompanied with an arithematic unit

and a display system, and a data read-out device. The analyzer cycle in the TOF analysis is initiated by a trigger pulse (T_z) derived from the LINAC. Time analysis is usually carried out with a time channel width of 20 (or 10)μs and an overflow channel number 512 (or 1024). The channel width is a dominant factor of the resolution for a large Q, and it should be adjusted to be sufficiently narrow for the measurement of structure factors for a large Q region.

3. 5 Sample Container

The sample container used in our experiments is a thin-walled cylindrical quartz vessel: 100mm in length, 10mm internal diameter and 0.1 mm wall thickness. The container possesses the following advantages in diffraction experiments on liquids:

(a) Quartz is a well-known resistant to corrosive materials; e. g., when concentrated acid solutions or organic liquids are left in a container for a considerable length of time no corrosive effect is observed.

(b) The thin wall-width of the container keeps the scattering intensity from it at a minimun, and the effect of the background counting from the container is negligibly small in the case of the measurements of samples with a moderate scattering cross -section such as deuterium oxide.

(c) The container can be used for experiments at more elevated temperatures than room temperature. Difference of intensities scattered from the empty container between different temperatures are negligibly small and this is also attributed to its thin wall-thickness.

3. 6 Temperature Control System

Neutron scattering experiments were frequently carried out on the samples, which were maintained at high or low temperatures and pressures, or in a magnetic field, etc. In such cases, in addition to the problem of the sample container as stated in the preceding section, appropriate devices and techniques are required. We discuss here only a temperature control system used for the diffraction experiments with increasing temperatures.

In the temperature control system, the vertical axis of the heating rod and that of the sample container are placed exactly at the two focussing points of a thin aluminum cylindrical reflector of an elliptical contour (major axis=200 mm, minor axis= 176 mm and height=220 mm (Fig. 2)). The sample is heated up by radiation converging on the focus within the reflector. An auxilliary heater of a planar type is set underneath the sample. Temperature measurement is made by CA thermocouples inserted into the top and bottom of the sample. Temperature control is performed by a Digital Thermometer (FLUKE Model 2190A) connected with a Thermocouple Multipoint Selector (FLUKE Model Y2001). The temperature is controlled within the fluctuation of 1℃ over the measuring time.

4. Experimental Resolution and Accuracy

We discuss here the overall experimental resolution and accuracy of the instrumental setup described in the preceding sections.

4. 1 Resolution

The fractional resolution $\Delta Q/Q$ is expressed as

$$\frac{\Delta Q}{Q}=\left[(\Delta\theta\cot\theta)^2+\left(\frac{\Delta t}{t}\right)^2+\left(\frac{\Delta \ell}{\ell}\right)^2\right]^{\frac{1}{2}} \tag{4}$$

where $\Delta\theta$, Δt and $\Delta \ell$ represent the uncertainties in θ, t and ℓ, respectively. $\Delta\theta$ is attributed to the widening of the incident beam $\Delta\theta_1$ and that of the scattered one $\Delta\theta_2$. $\Delta\theta_1$ is determined by the slit width of the pre-collimator and the widening of the beam along the path between the source and the sample. $\Delta\theta_1$ in the present geometry becomes about 51′. $\Delta\theta_2$ is mainly determined by the slit width of the Soller collimator. The magnitude of $\Delta\ell$ is calculated from the effective radius of the radiation surface of the neutron source and the diameters of sample and detector, and is estimated to be ca. 8cm. Δt is determined from the pulse width τ_p of electron burst in LINAC, the mean-emission-time τ_m at the moderator and the channel width τ_c in the multi-channel time analyzer.

Fig. 4 shows the values of $\Delta Q/Q$ calculated for the case of $\tau_p=3\mu$s, $\tau_c=20\mu$s and $\Delta\theta_2=30'$, using the values of τ_m given in Fig. 3. The broad and weak rise appears in $\Delta Q/Q$ curves for the range of $Q<20$ Å.$^{-1}$ This is attributed to the steep increase of the mean-emission-time for the range of $E=0.1-0.3$eV as seen in Fig. 3. The resolution over a wide-Q range is found to be less than a few % at higher scattering angles. As seen in the figure, the sufficiently narrow channel width of the multi-channel time analyzer should be set up when the improvement of $\Delta Q/Q$ for a larger Q region is required. The monotonous increase in larger Q region results from the relatively large channel width against the total time-of-flight. The large magnitude of $\Delta Q/Q$ at lower scattering angles ($2\theta=20°$ and 40°) are attributed to the widening of the slit width of collimators mainly.

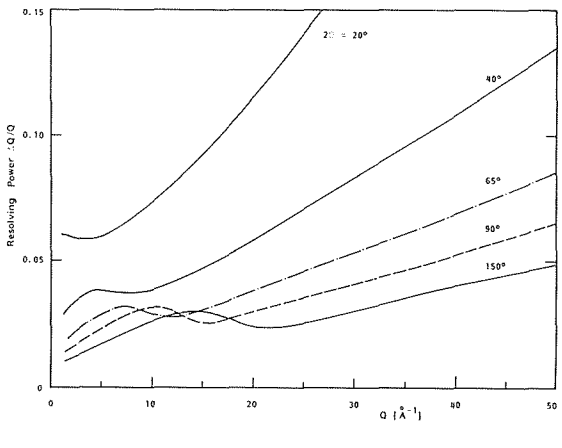

Fig. 4. Resolving power $\Delta Q/Q$ at various scattering angles.

4. 2 Intensity

The scattering intensity obtained in the LINAC-TOF neutron diffraction measur-

ement is governed by a number of factors. They are classified into two groups of easily variable factors and invariable ones. The former are the repetition rate of electron burst r_p, the pulse width of the burst τ_p, the channel width of multi-channel time analyzer τ_c, the measuring time T and the operating voltage of detector V influencing the detector efficiency. The latter are the factors associated with the source intensity spectrum and the transmission for collimators. etc. Under a given condition with respect to the latter factors. for example, measured intensity for a sample of deuterium oxide at $2\theta=90°$ is 6,000 counts per channel for neutrons of $\lambda=2$ Å when $r_p=100$ pps, $\tau_p=3\,\mu$s, $\tau_c=20\,\mu$s, $T=30$ min. and $V=1700$ volts. Summing up the counts for channels within the resolving power, the statistical error becomes less than 0.5% over the whole range of Q covered for an acceptable count-rate of neutrons (Fig. 1).

5. Data Processing

In the TOF neutron diffraction experiment on liquid samples, five different runs are necessary to be carried out at each scattering angle for (1) sample in the container, (2) empty container, (3) background scattering by air, (4) vanadium rod and (5) poly-crystalline material. In order to obtain the structure factor from measured intensity data, a number of corrections must be applied to the scattering data by the sample, by the container and by the vanadium rod, and thereafter several normalizations and calibrations are carried out.

As a consequence of laborious and tedious procedures of the data reduction in addition to the accumulation of large amount of raw data, it becomes necessary to turn to the methods of analysis using an electronic computer. A flow diagram of the data reduction program is shown in Fig. 5, where only the case of measurements at two scattering angles is indicated.

5. 1 Corrections for Background, Absorption and Multiple Scattering

In the first step, corrections for background counting, absorption and multiple scattering are considered, and these corrections can be performed experimentally and theoretically. In our present procedure of data reduction, the theoretical methods are applied to absorption and multiple scattering effects as well as the inelastic scattering effect described below.

The relation between the raw data ($B_i(t)$, $V_i(t)$, $C_i(t)$ and $S_i(t)$) and the intensity corrected for the absorption, multiple scattering and background ($I_{ji}(t)$) is given by

$$I_{Si}(t)=\frac{1}{A_{s,sc}(t)}\left[S_i(t)-C'_i(t)-\frac{A_{c,sc}(t)}{A_{c,c}(t)}\{C_i(t)-B'_i(t)\}\right]-I''_{Si}(t) \tag{5}$$

and

$$I_{Vi}(t)=\frac{1}{A_{V,V}(t)}\left[V_i(t)-B'_i(t)\right]-I''_{Vi}(t), \tag{6}$$

where $A_{\alpha,\beta\gamma}$ terms are the notation for cylindrical absorption factor by Paalman and

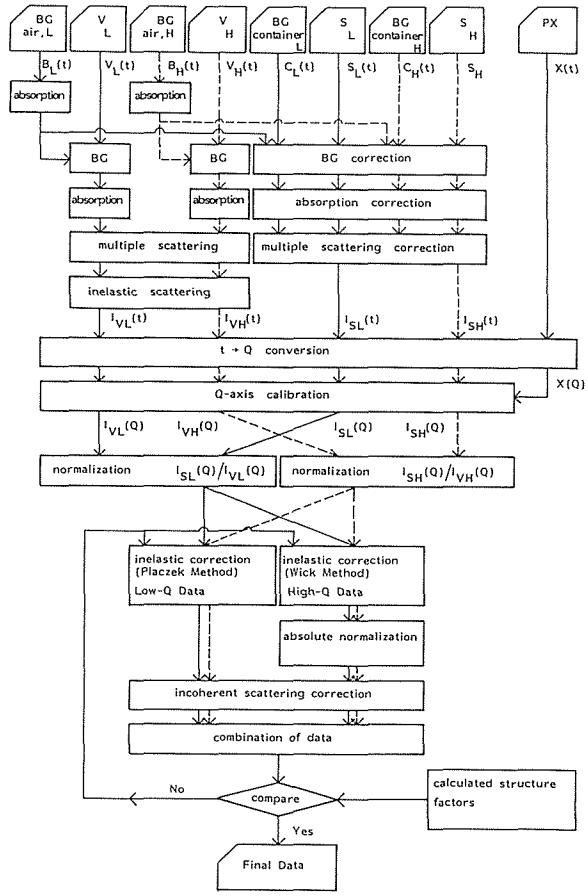

Fig. 5. Flow diagram of the data reduction program.
$S_i(t)$: neutron-scattering intensity for a sample filling the container (S), $V_i(t)$: neutron-scattering intensity for vanadium (V), $B_i(t)$: background intensity by air scattering (BG_{air}), $C_i(t)$: background intensity for the empty container ($BG_{container}$), $X(t)$: neutron-scattering intensity for poly-crystalline materials (PX), $I_{Vi}(t)$: fully-corrected neutron-scattering intensity for vanadium, $I_{Si}(t)$: neutron-scattering intensity for the sample after corrected with respect to multiple scattering, absorption and background scattering, $I_{Vi}(Q)$: neutron-scattering intensity for vanadium after $t \rightarrow Q$ conversion and Q-axis calibration. $I_{Si}(Q)$: neutron-scattering intensity for the sample after $t \rightarrow Q$ conversion and Q-axis calibration. Suffix i is L and H which denotes lower and higher scattering angle, respectively.

Pings[8] $B'_i(t)$ and $C'_i(t)$ the duely corrected background intensity, $I''_{ji}(t)$ the calculated multiple scattering intensity (other notations are described in the figure caption of Fig. 5).

With respect to the correction for the multiple scattering, we use Blech and Averbach's method,[9] where the scattering is assumed to be isotropic and the effect of

double scattering only is taken into consideration. The multiple scattering intensity $I''_{ji}(t)$ is calculated by the formula $I''_{ji}(t)=I_0[(\sigma_t-\sigma_a)/\sigma_t]\delta$, where σ_t and σ_a are the total and absorption cross-section, respectively, I_0 the isotropic total scattering intensity and δ is a geometrical factor determined by the shape and dimensions of the sample.[9] We apply this method to the scattering data of the sample and those of the vanadium rod.

5. 2 Correction for Inelastic Scattering

We have observed a steady fall in structure factor curves with the increasing Q, which is caused by the inelastic scattering of neutrons by light nuclei. The correction for the inelastic scattering is the most important for hydrogenous molecular liquids like deuterium oxide. For compensating the effect, several conventional and useful correction methods have been used so far. Powles[10] has proposed the method of the Placzek correction[11] for the TOF diffraction method using the LINAC pulsed neutrons. Matsumoto[12] has also applied the Wick method[13] to the LINAC-TOF neutron diffraction experiment. There exist some semi-empirical schemes for applying these correction methods, but no more rigorous numerical procedure applicable over a wide range of Q has been discovered. Thus, we have applied these two methods complementally to the analysis in our studies as in the following.

In the Placzek method, the dynamical structure factor $S(Q, \omega)$ is expanded in the power series of m/M, where m and M are the mass of neutron and the effective mass of scatterer, respectively. For the case $M>>m$, the correction is usually only a few per cent and the first few terms of the Placzek expansion appear to be sufficient. The formalism in the TOF experiment given by Powles, in a first approximation neglecting the correction on the distinct terms, is expressed as

$$\frac{d\sigma}{d\Omega}\Big|_{exp} \propto \frac{I_{si}(Q)}{I_{vi}(Q)} \propto 1-2\left(\frac{m}{M}\right)\sin^2\theta\times C \tag{7}$$

where C is a factor determined by the geometrical arrangement of the diffractometer, the detector efficiency and the neutron source spectrum. The effective mass is roughly assumed to be inversely proportional to Q. For the case of a constant neutron spectrum in wavelength (C : constant), introducing the relation of $m/M \propto Q$ into Eq. 7, we obtained $d\sigma/d\Omega_{exp} \propto 1-Q\sin^2\theta\times C$. This result explains a typical feature of the Placzek correction, that is, the greater descending trend in structure factor curves with the increasing Q is seen, which is observed in a low Q region at larger scattering angle. Accordingly, the Placzek method is safely applicable to data for low Q region.

The Wick method is based on the expansion of the intermediate scattering function $\chi(Q, t)$ in powers of t, where t is the duration of a collision which is sufficiently short, compared with the characteristic periods of atomic motions. The Wick formalism in the TOF experiment by Matsumoto is expressed as

$$\frac{d\sigma}{d\Omega}_{exp} \propto \frac{I_{si}(Q)}{I_{vi}(Q)} \propto \sum_{n=0}^{3} P_n(Q^{-2})^n \tag{8}$$

where P_n is a parameter which is independent of Q. An important feature of the

result is that it removes the restriction of small m/M required for the Placzek method. This indicates that the Wick method is useful for the compensation of the inelastic effect by light nuclei. Furthermore, the Q-dependence of Eq. 8 explains the trend in structure factor curves in a high Q region, and the Wick method is also applicable to data for high Q region.

Thus, the Placzek correction method can be used in a low Q region and the Wick correction method in a high Q region (Fig. 5). In our recent studies on liquid deuterium oxide, acetyle chloride, etc., we have applied a complementary combination procedure of the Placzek and the Wick methods successfully.[1~5]

5. 3 Absolute Normalization and Calibration

Absolute normalization of data is carried out using the scattering data from a poly-crystalline vanadium rod of the same shape and dimensions as those of the sample. Vanadium is regarded as an isotropic and incoherent scatterer. Subsequently, calibration of the absolute scale of structure factor data is carried out as follows: calibration of high Q data is made according to the limiting procedure that $S_m(Q) \rightarrow \Sigma b_n^2/(\Sigma b_n)^2$ as $Q \rightarrow \infty$, where b_n is the coherent scattering length for n-th nucleus and n ranges over all the nuclei in a molecule, and calibration for low Q data is done by overlapping the structure factor curves in a due Q range for the two corrected data. In this calibration procedure, the correction for incoherent scattering is duely considered.

In the final stage of the data reduction, the combination of data is carried out as in the following. First, in order to obtain the structure factor curve for a wide range of Q at a scattering angle, we combine the two fully-corrected data at each scattering angle. Next, combining these data at two angles, the final structure factor curve is obtained. Finally, gradual refinement of the final curve is made by an iterative procedure where the observed curve is compared with an unchanged part of the total and intramolecular structure factor curves calculated for an appropriate structure model.

5. 4 Calibration of Q-Scale

The scale of momentum transfer Q is calibrated from well resolved Bragg reflection peaks in the diffraction pattern from poly-crystalline materials such as copper, germanium, etc. The scattering from the crystal is limited to the values of scattering vector $\vec{Q}$ equal to the set of reciprocal lattice vector $\vec{\tau}$, and the magnitude $|\vec{\tau}| = 2\pi/d$ is inversely proportional to the plane spacing d. Thus, the scattering can occur only at the values of λ given by the Bragg equation, $\lambda = 2d\sin\theta$. Combining this equation with Eq. 2, we can determine correct values of Q from the Bragg peaks. In addition, the full-width of half-maximum (FWHM) of Bragg peaks is also used for an estimation of the overall resolution of the TOF diffraction instruments. In that case, it must be noted that the widening of the FWHM is attributed, in part, to the crystal deformation.[14]

6. Concluding Remarks

The time-of-flight neutron diffraction equipment at Hokkaido University was mainly intended for the study of structure of liquids, solutions and amorphous materials. The whole experimental setup is constructed of the following subdivisions: pulsed -neutron source, TOF neutron diffractometer, neutron counting system and data processing unit, including a temperature control system. Measured TOF data must be subjected to a series of corrections (background, absorption, multiple scattering, inelastic scattering and incoherent scattering), normalizations, and calibrations. We have given a detailed description of the instrumentation and data reduction procedures. These instruments and procedures have proved to be quite useful for structural studies of liquids through the applications to various molecular liquids and solutions, which have been carried out by the authors' group.[1~5,15,16]

In order to carry out the structural study of the fluid system by means of the LINAC-TOF neutron diffraction, a general theoretical procedure of analysis is required, in addition to the experimental setup and the data processing procedure described in the present paper. Recently, the authors' group has succeeded in giving a general theory of analysis for the fluid system composed of molecular clusters with various sizes, and analyzed the structure factor data for D_2O at 15~95℃ by using a general expression of $S_m(Q)$ derived from the theory. The structure of liquid water has been determined from the excellent agreement between calculated and observed structure factors. The details of the theory and the results are reported in *Bull. Chem. Soc. Jpn.*[15,16]

References

1) N. Ohtomo and K. Arakawa, *Bull. Chem. Soc. Jpn.*, **51**, 1649 (1978).
2) N. Ohtomo and K. Arakawa, *Bull. Chem. Soc. Jpn.*, **52**, 2755 (1979).
3) N. Ohtomo and K. Arakawa, M. Takeuchi, T. Yamaguchi and H. Ohtaki, *Bull. Chem. Soc. Jpn.*, **54**, 1314 (1981).
4) N. Ohtomo and K. Arakawa, *Bull. Chem. Soc. Jpn.*, **53**, 1789 (1980).
5) N. Ohtomo and K. Arakawa, *Bull. Chem. Soc. Jpn.*, **53**, 1510 (1980).
6) N. Ohtomo and K. Inoue, *Bull. Faculty Eng. Hokkaido Univ.*, **73**, 105 (1974).
7) N. Ohtomo and K. Inoue, *J. Nucl, Sci. Technol.*, **12**, 384 (1975).
8) H. H. Paalman and C. J. Pings, *J. Appl. Phys.*, **33**, 2635 (1962).
9) I. A. Blech and B. L. Averbach, *Phys. Rev.*, **137**, A1113 (1965).
10) J. G. Powles, *Mol. Phys.*, **26**, 1325 (1973); **36**, 1181 (1978), etc.
11) G. Placzek, *Phys. Rev.*, **86**, 377 (1952).
12) T. Matsumoto, *J. Nucl. Sci. Technol.*, **16**, 401 (1979).
13) G. C. Wick, *Phys. Rev.*, **94**, 1228 (1954).
14) N. Ohtomo and H. Iwasa, *Bull. Faculty Eng. Hokkaido Univ.*, **88**, 77 (1978).
15) N. Ohtomo, K. Tokiwano and K. Arakawa, *Bull. Chem. Soc. Jpn.*, **54**, 1802 (1981).
16) N. Ohtomo, K. Tokiwano and K. Arakawa, *Bull. Chem. Soc. Jpn.*, to be published.